Supporting Information

Lanthanide-MOFs based Host-guest Intelligent Dual-Stimulus Response Platform for Naked-eye and Ratiometric Fluorescent Monitoring of Food Freshness

Chengshan Ji[a], Jian Zhang[a]*, Ruiqing Fan[a]*, Yinan Chen[a], Yifan Zhang[a], Tiancheng Sun[a], and Yulin Yang[a]*

MIIT Key Laboratory of Critical Materials Technology for New Energy Conversion and Storage, School of Chemistry and Chemical Engineering, Harbin Institute of Technology, Harbin 150001, P. R. of China

Corresponding Author: * Jian Zhang, Ruiqing Fan, and Yulin Yang

E-mail: zhaji@hit.edu.cn, fanruiqing@hit.edu.cn and ylyang@hit.edu.cn

Contents

Experimental section

Chemicals and Measurements

All chemicals were commercially available reagents of analytical grade and were used without further purification. The 5-((4'-(imidazol-1-yl)benzyl)oxy)isophthalic acid (H_2dbia) ligand were purchased from Jinan Henghua Sci. & Tec. Co. Ltd (Shandong, China). All the lanthanide metal salts $Ln(NO_3)_3 \cdot 6H_2O$ (Ln= Sm, Eu) were purchased from Innochem. Besides, all the detected substances and interferences, fluorescein (flu), tyramine (Tyr), spermine (spe), putrescine (put), cadaverine (cad), tryptamine (try), histamine (his), ascorbic acid (asc), cysteine (cys), adenine (ade) and histidine (hid) were also purchased from Innochem company.

The FT-IR spectra were obtained from KBr pellets using a Nicolet Avatar-360 infrared spectrometer in the 4000 ~ 400 cm^{-1} region. The thermal analyses were performed on a STA 449 F5 Jupiter thermogravimetric analyzer from 30 °C to 750 °C with a heating rate of 10 °C min^{-1} in air atmosphere. Powder X-ray diffraction (PXRD) patterns were recorded in the 2θ range of 5° ~ 50° using Cu-Kα radiation with a Shimadzu XRD-6000 X-ray diffractometer. The simulation of PXRD pattern was carried out using the single-crystal data and diffraction-crystal module of the Mercury (Hg) program version 3.0. UV-vis spectra were obtained on an Agilent Cary 60spectrometer. All the luminescent measurements were recorded on an Edinburgh FLS 920 fluorescence spectrometer in the range of 450 ~ 750 nm. Time-resolved luminescent decay curves are well fitted into a mono-exponential function: $I_0 = I + A \exp(-t/\tau)$, where I and I_0 are the luminescent intensities at time $t = t$ and $t = 0$, whereas τ is defined as the luminescent lifetime. All the DFT calculation were carried out at the B3LYP/6-31 G* level of Gauss 09 program. The calculation formula of loading content of Flu is as follows: Flu loading content % = $\frac{m_{(Flu@Eu-dbia)} - m_{(Eu-dbia)}}{m_{(Flu@Eu-dbia)}} \times 100\%$, where $m_{(Eu-dbia)}$ and $m_{(Flu@Eu-dbia)}$ is calculated by the final weight loss of Eu-dbia and Flu@Eu-dbia.

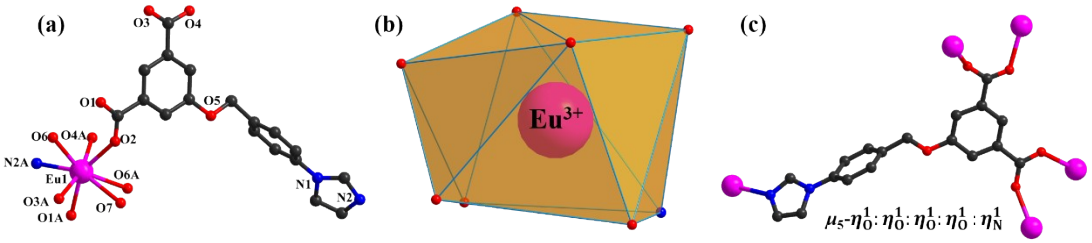

Fig. S1 (a) The asymmetric structural unit of Eu-dbia. (b) The Twisted bi-capped triangular prismatic geometries of Eu1. (c) The coordination mode of coordinated $dbia^{2-}$ ligands in Eu-dbia.

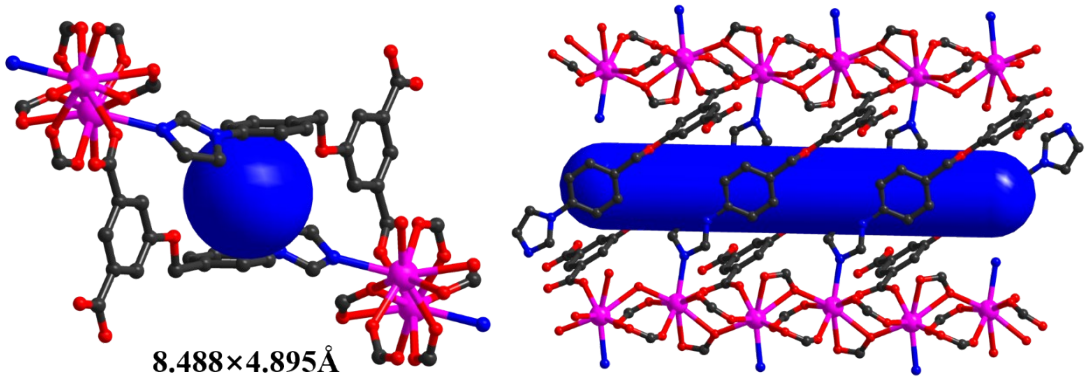

Fig. S2 The rectangle channel of Eu-dbia and its side view.

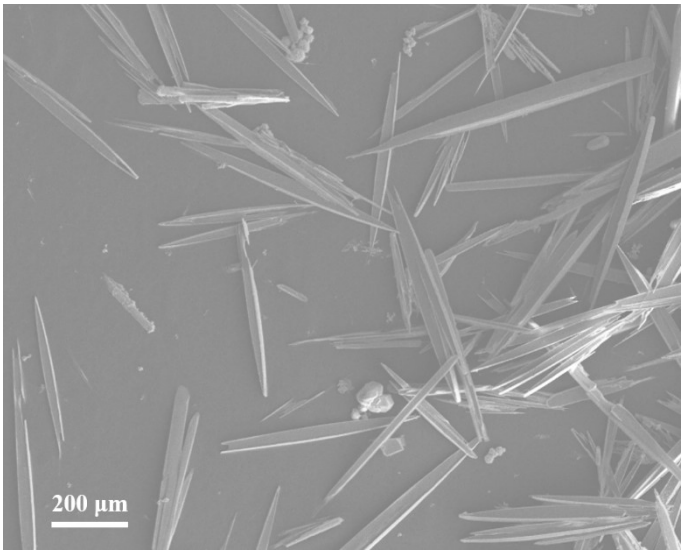

Fig. S3 The SEM image of Eu-dbia.

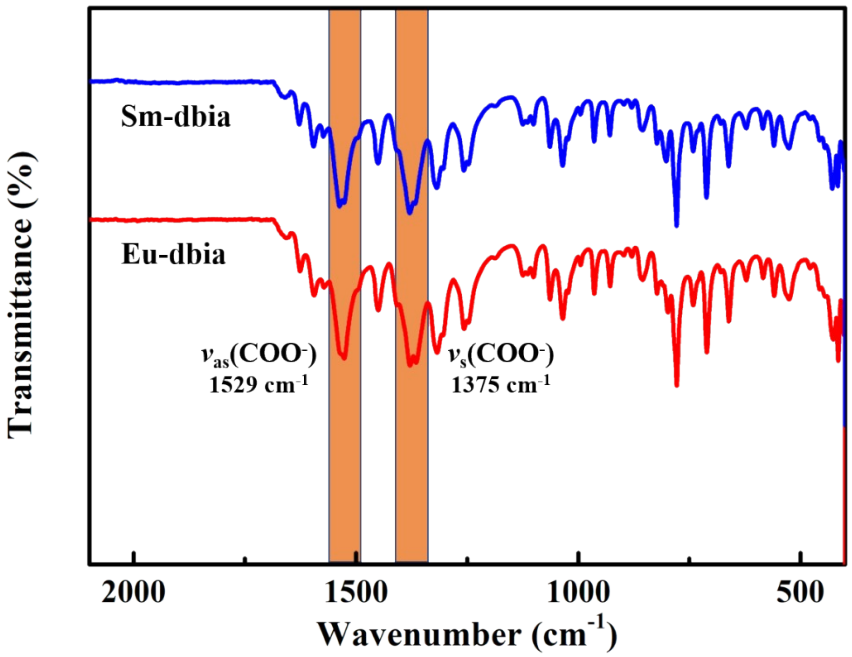

Fig. S4 FTIR spectra of Ln-dbia.

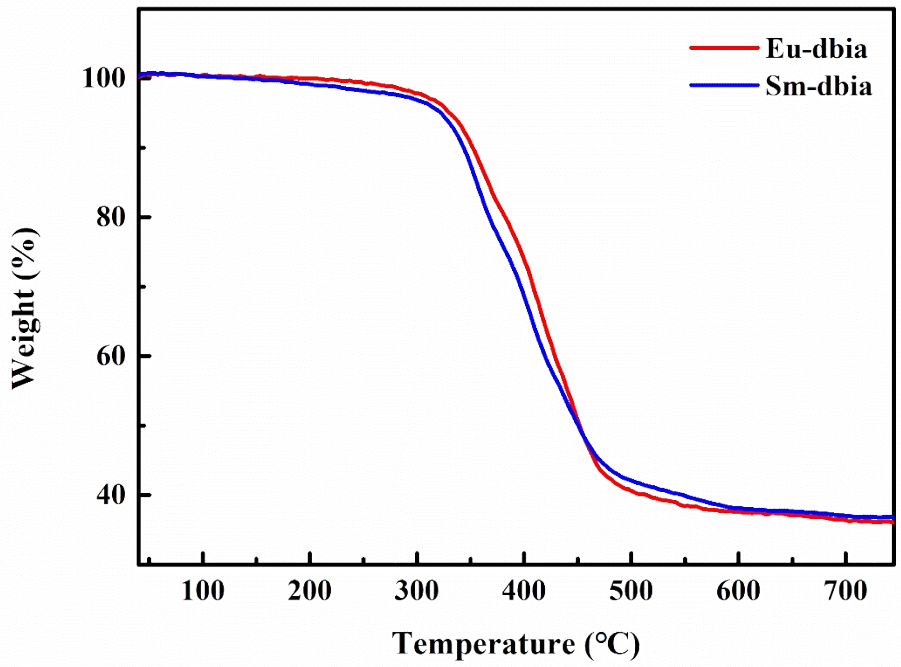

Fig. S5 TGA of Ln-dbia.

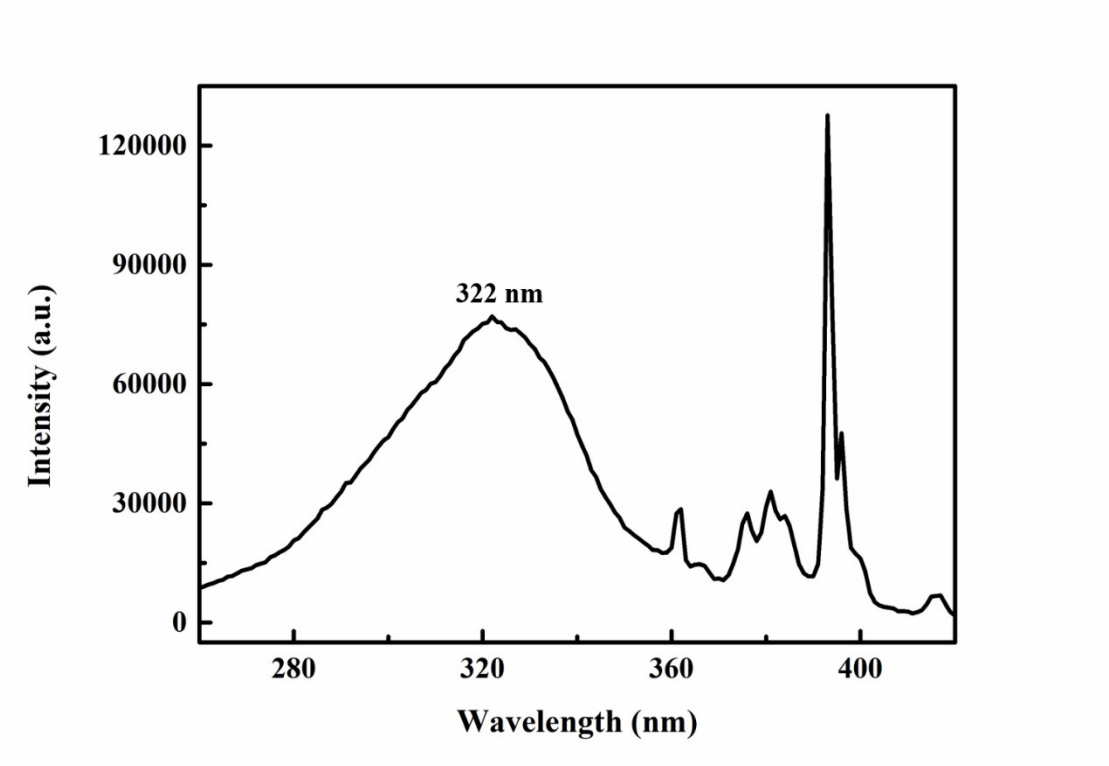

Fig. S6 Excitation spectra of Eu-dbia.

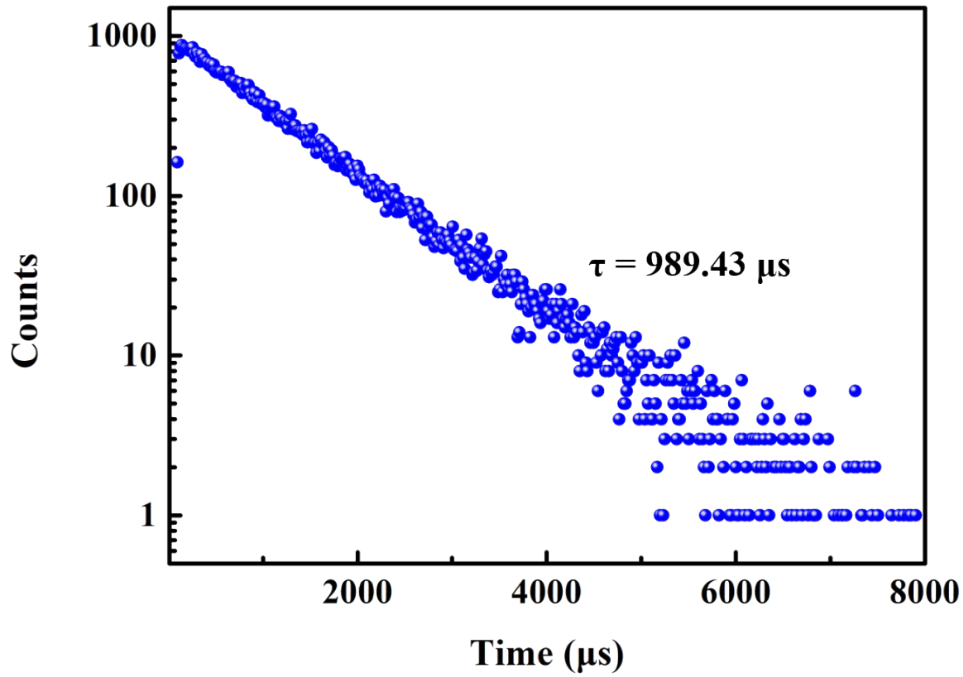

Fig. S7 Luminescent decay curves of Eu-dbia.

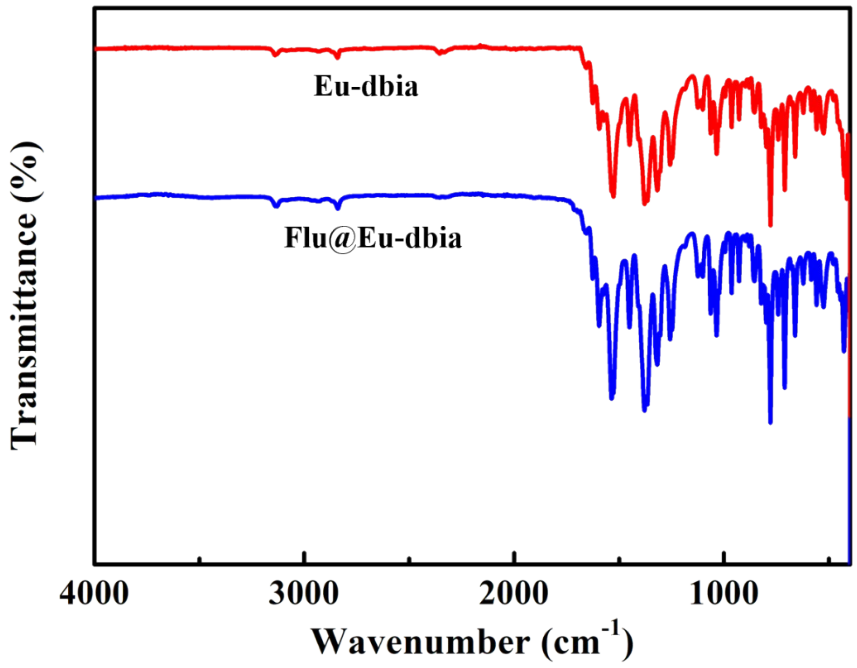

Fig. S8 FTIR spectra of Eu-dbia and Flu@Eu-dbia.

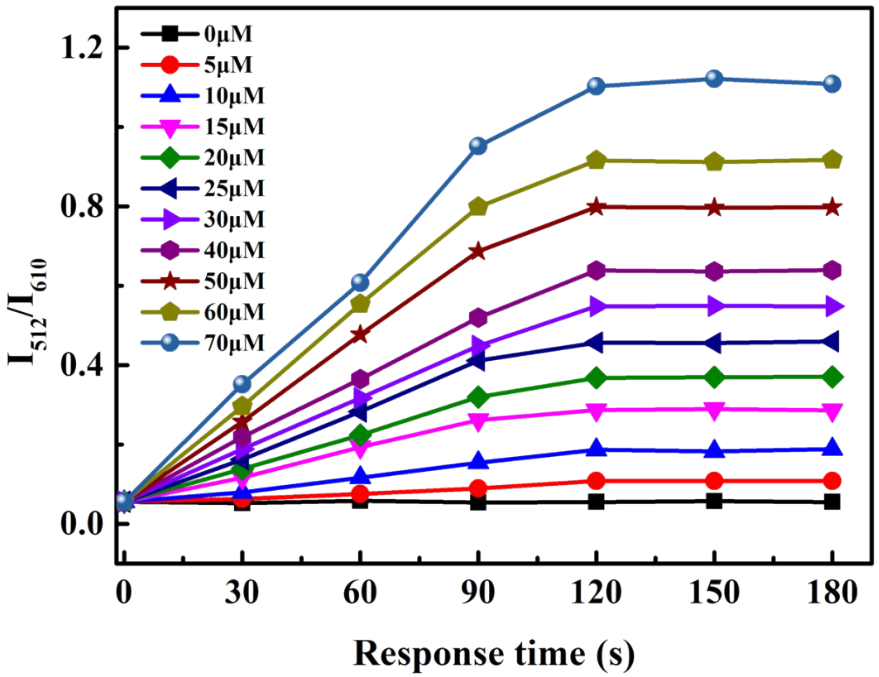

Fig. S9 Fluorescence emission intensity of I_{512}/I_{610} in different time (0 ~ 180 s) upon exposure to different concentrations of Tyr.

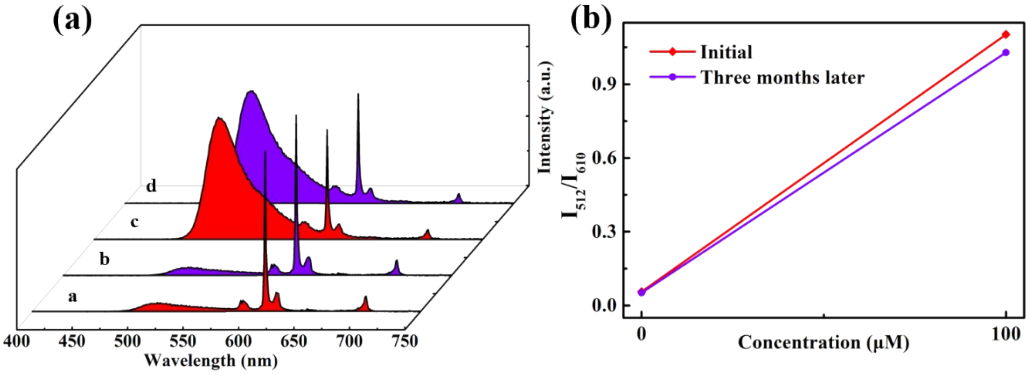

Fig. S10 (a) Fluorescence spectra of Flu@Eu-dbia at initial and three months later (a: initial, b: three months later; c: initial and d: three months later treated with 100 μM Tyr). (b) Corresponding fluorescence intensity ratio of (I_{512}/I_{610}).

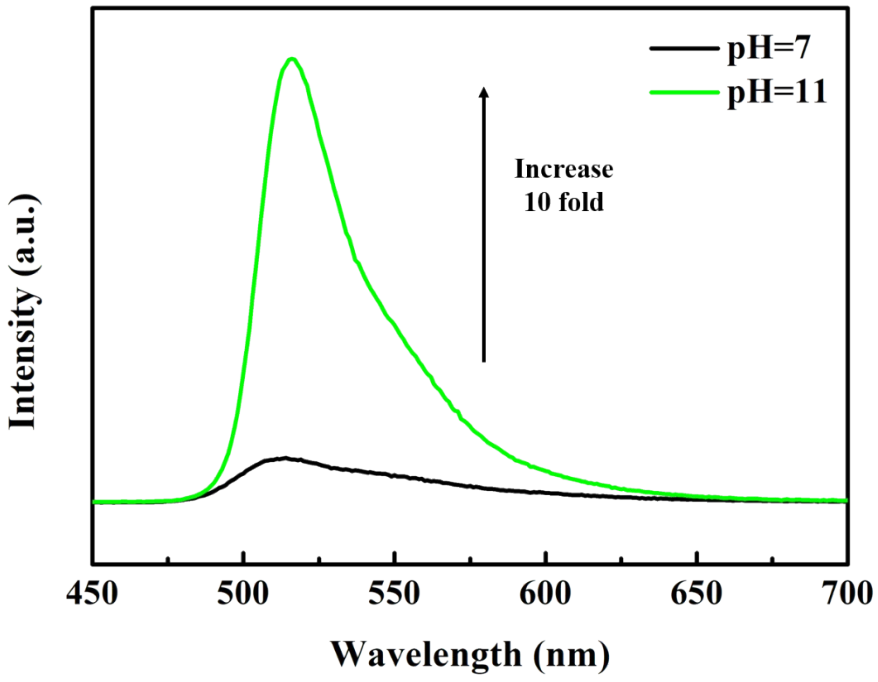

Fig. S11 Fluorescence spectra of Flu in different pH aqueous solutions.

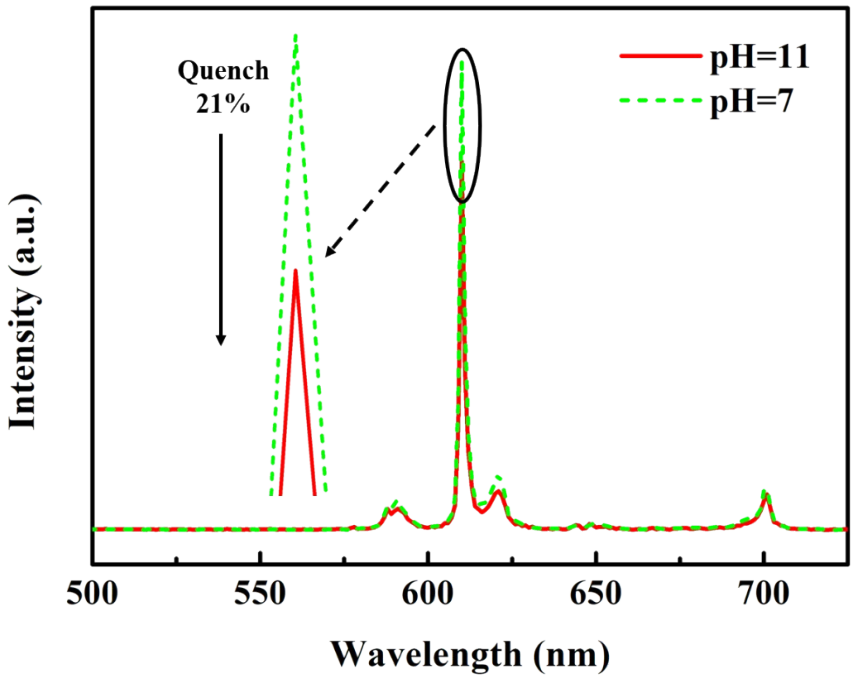

Fig. S12 Fluorescence spectra of Eu-dbia in different pH aqueous solutions.

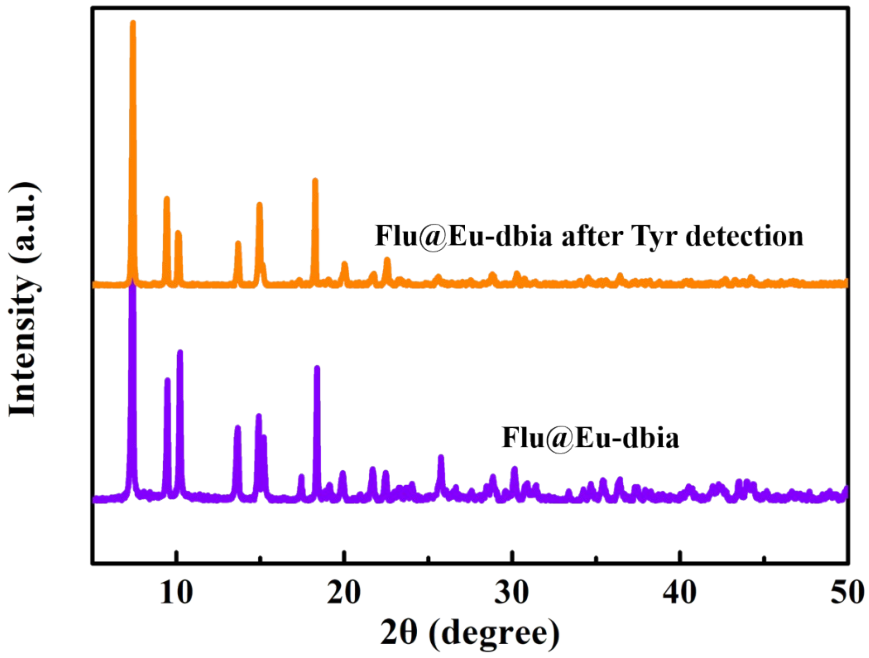

Fig. S13 PXRD patterns of Flu@Eu-dbia after Tyr detection.

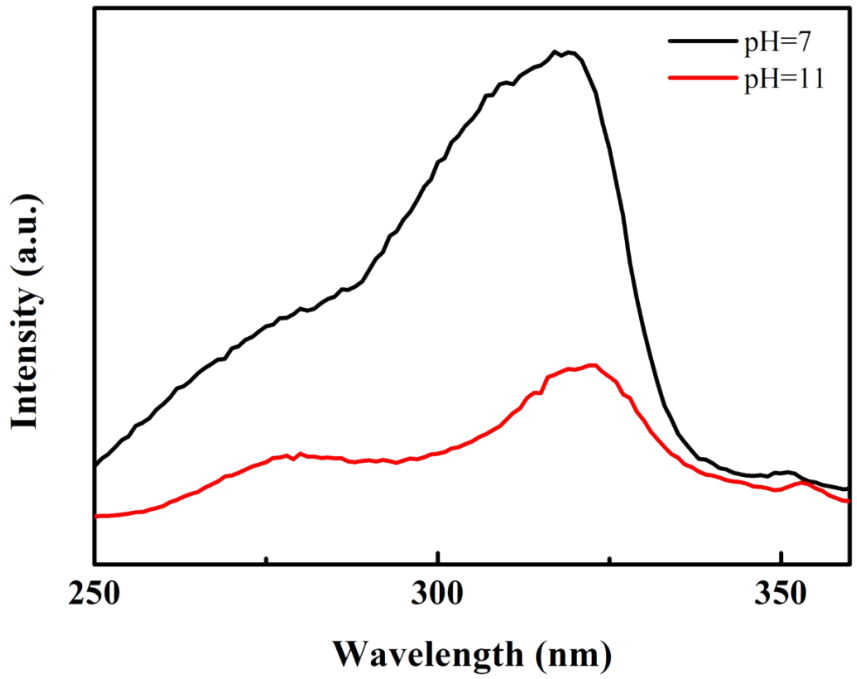

Fig. S14 Excitation spectra of the H_2dbia ligand in different pH aqueous solutions.

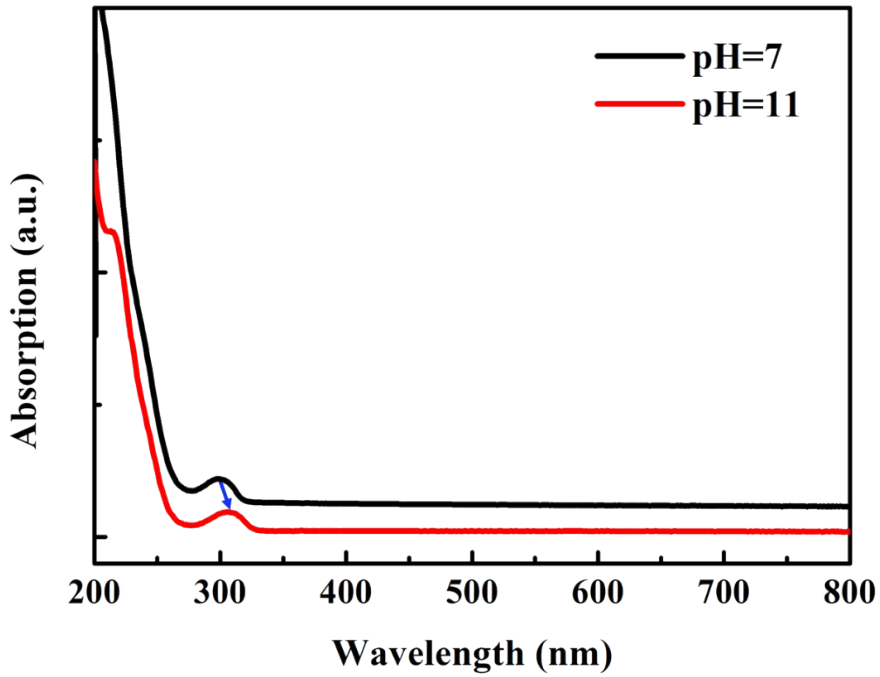

Fig. S15 UV-vis absorption spectra of Eu-dbia in different pH aqueous solution.

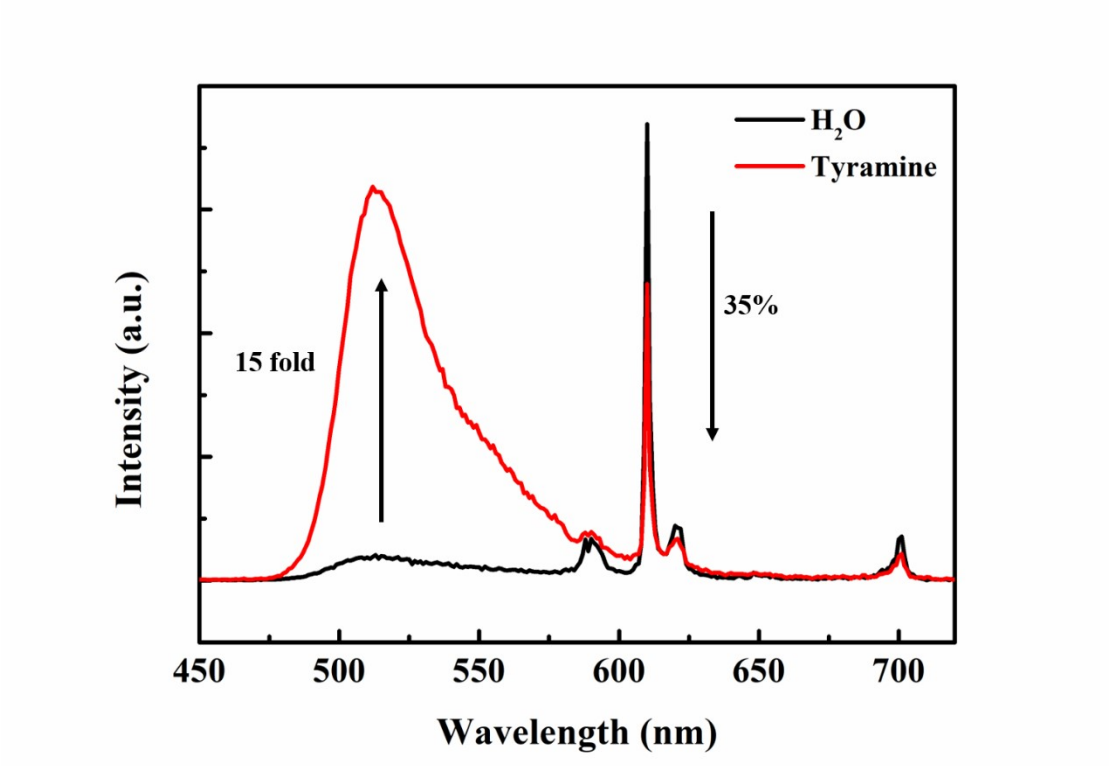

Fig. S16 Fluorescence spectra of Flu@Eu-dbia in different pH aqueous solutions.

Table S1 Crystallographic data and structural refinements for Sm-dbia and Eu-dbia.

		Sm-dbia	**Eu-dbia**
Empirical formula		$C_{19}H_{12}SmN_2O_7$	$C_{19}H_{12}EuN_2O_7$
Formula weight		530.66	532.27
Crystal system		Monoclinic	Monoclinic
Space group		C2/c	C2/c
a/Å		24.5539(16)	24.6008(12)
b/Å		8.2544(5)	8.2296(4)
c/Å		19.4085(11)	19.3862(8)
α (°)		90	90
β (°)		107.351(2)	107.132(2)
γ (°)		90	90
Volume/Å^3		3754.7(4)	3750.7(3)
Z		8	8
D_{calcd}/Mg·m^{-3}		1.878	1.885
μ/mm^{-1}		3.173	3.39
F(000)		2064	2072
θ range (°)		2.616 – 25.000	2.622 –24.783
Limiting indices		-29≤h≤29 –9≤*k*≤9 –23≤*l*≤23	-28≤h≤28 –9≤*k*≤9 –20≤*l*≤22
GOF on F^2		1.129	1.269
Final *R* indices	R_1 [a]	0.0546	0.0411
[$I > 2\sigma(I)$]	wR_2 [b]	0.1320	0.0971
R indices	R_1	0.0587	0.0452
(all data)	wR_2	0.1338	0.0989
CCDC		2207231	2207229

[a] $R_1 = \sum||F_o| - |F_c||/\sum|F_o|$. [b] $wR_2 = \{\sum[w\,(F_o^2 - F_c^2)^2]/\sum[\,w\,(F_o^2)^2]\}^{1/2}$

Table S2 Selected bond lengths (Å) and bond angles (°) for Sm-dbia.

Bond	Bond Lengths (Å)	Bond	Bond Lengths (Å)
Sm(1)-O(3)#1	2.358(7)	Sm(1)-O(7)#3	2.408(7)
Sm(1)-O(4)#2	2.367(6)	Sm(1)-O(6)	2.555(9)
Sm(1)-O(1)	2.376(6)	Sm(1)-O(7)	2.558(8)
Sm(1)-O(2)#3	2.380(6)	Sm(1)-N(2)#4	2.580(10)
Bond	Bond Angles (°)	Bond	Bond Angles (°)
O(3)#1-Sm(1)-O(4)#2	164.8(3)	O(7)#3-Sm(1)-O(6)	126.4(3)
O(3)#1-Sm(1)-O(1)	107.0(3)	O(3)#1-Sm(1)-O(7)	73.5(3)
O(4)#2-Sm(1)-O(1)	76.6(2)	O(4)#2-Sm(1)-O(7)	121.3(3)
O(3)#1-Sm(1)-O(2)#3	77.6(2)	O(1)-Sm(1)-O(7)	73.1(2)
O(4)#2-Sm(1)-O(2)#3	107.2(2)	O(2)#3-Sm(1)-O(7)	79.4(2)
O(1)-Sm(1)-O(2)#3	149.1(3)	O(7)#3-Sm(1)-O(7)	153.21(8)
O(3)#1-Sm(1)-O(7)#3	92.2(3)	O(6)-Sm(1)-O(7)	51.0(3)
O(4)#2-Sm(1)-O(7)#3	75.5(2)	O(3)#1-Sm(1)-N(2)#4	71.5(3)
O(1)-Sm(1)-O(7)#3	133.5(3)	O(4)#2-Sm(1)-N(2)#4	96.1(3)
O(2)#3-Sm(1)-O(7)#3	75.4(3)	O(1)-Sm(1)-N(2)#4	72.9(3)
O(3)#1-Sm(1)-O(6)	119.8(3)	O(2)#3-Sm(1)-N(2)#4	135.0(3)
O(4)#2-Sm(1)-O(6)	75.2(3)	O(7)#3-Sm(1)-N(2)#4	74.0(3)
O(1)-Sm(1)-O(6)	80.0(3)	O(6)-Sm(1)-N(2)#4	152.8(3)
O(2)#3-Sm(1)-O(6)	71.9(3)	O(7)-Sm(1)-N(2)#4	120.2(3)

Table S3 Selected bond lengths (Å) and bond angles (°) for Eu-dbia.

Bond	Bond Lengths (Å)	Bond	Bond Lengths (Å)
Eu(1)-O(4)#1	2.342(5)	Eu(1)-O(6)	2.551(5)
Eu(1)-O(3)#2	2.358(5)	Eu(1)-N(2)#5	2.569(7)
Eu(1)-O(1)#3	2.365(5)	Eu(1)-O(6)#4	2.406(5)
Eu(1)-O(2)	2.370(5)	Eu(1)-O(7)	2.541(6)
Bond	Bond Angles (°)	Bond	Bond Angles (°)
O(4)#1-Eu(1)-O(3)#2	164.5(2)	O(6)#4-Eu(1)-O(6)	153.24(5)
O(4)#1-Eu(1)-O(1)#3	107.5(2)	O(7)-Eu(1)-O(6)	50.96(19)
O(3)#2-Eu(1)-O(1)#3	76.81(18)	O(4)#1-Eu(1)-N(2)#5	71.5(2)
O(4)#1-Eu(1)-O(2)	77.11(19)	O(3)#2-Eu(1)-N(2)#5	96.2(2)
O(3)#2-Eu(1)-O(2)	107.2(2)	O(1)#3-Eu(1)-N(2)#5	72.8(2)
O(1)#3-Eu(1)-O(2)	149.0(2)	O(2)-Eu(1)-N(2)#5	135.1(2)
O(4)#1-Eu(1)-O(6)#4	91.72(19)	O(6)#4-Eu(1)-N(2)#5	74.1(2)
O(3)#2-Eu(1)-O(6)#4	75.35(19)	O(7)-Eu(1)-N(2)#5	152.5(2)
O(1)#3-Eu(1)-O(6)#4	133.54(19)	O(6)-Eu(1)-N(2)#5	120.1(2)
O(2)-Eu(1)-O(6)#4	75.56(18)	O(6)#4-Eu(1)-O(7)	126.5(2)
O(4)#1-Eu(1)-O(7)	120.1(2)	O(4)#1-Eu(1)-O(6)	73.89(19)
O(3)#2-Eu(1)-O(7)	75.1(2)	O(3)#2-Eu(1)-O(6)	121.4(2)
O(1)#3-Eu(1)-O(7)	79.7(2)	O(1)#3-Eu(1)-O(6)	73.05(18)
O(2)-Eu(1)-O(7)	72.04(19)	O(2)-Eu(1)-O(6)	79.22(17)

Table S4 Comparison between the developed method and other methods for Tyr detection.

Materials	Method	LOD	References
Flu@Eu-dbia	fluorescence	66.3 nM	This work
FONs.Fe^{3+} complex	fluorescence	0.377 μM	[1]
$NaGdF_4$:Yb,Er@$NaYF_4$	fluorescence	26 nM	[2]
CDs-MIP test strips	fluorescence	0.43 μM	[3]
CS/LFO	electrochemical	0.6158 μM	[4]
Ty–SWCNT–COOH/SPE	electrochemical	0.62 μM	[5]
Ty/AuNPs/CNFs-IL-CH/GCE	electrochemical	93 nM	[6]

References

1. N. Kaur, M. Kaur, S. Chopra, J. Singh, A. Kuwar and N. Singh, *Food Chem.*, 2018, **245**, 1257-1261.
2. H. Wang, Y. Lu, L. Wang and H. Chen, *Talanta*, 2019, **197**, 558-566.
3. D. Qiao, Z. Zhang, L. Wang, W. Sheng, Q. Deng and S. Wang, *Microchem. J.*, 2021, **160**, 105638.
4. Pratibha, A. Kapoor and J. K. Rajput, *ACS Sustainable Chem. Eng.*, 2022, **10**, 11666-11679.
5. I. M. Apetrei and C. Apetrei, *J. Food Eng.*, 2015, **149**, 1-8.
6. P. E. Erden, C. Kaçar Selvi and E. Kılıç, *Microchem. J.*, 2021, **170**, 106729.